Article

In Vitro Detection of Biochemical Effect in Human CaCo-2 Cell Line after Exposure to a Low Concentration of a Deltamethrin-Based Pesticide

Giuseppe Perna ©, **Vito Capozzi** © and **Maria Lasalvia** * ©

Dipartimento di Medicina Clinica e Sperimentale, Università di Foggia, 71122 Foggia, Italy
* Correspondence: maria.lasalvia@unifg.it

Abstract: Pesticide residues are chemicals frequently found in food as contaminants. Pesticides may have adverse health effects, particularly when the digestive tract is concerned, as a consequence of food ingestion. Deltamethrin is a pyrethroid pesticide widely used in various fields, such as agriculture, veterinary and in the household, so the ingestion of a small amount of this chemical may occasionally occur. To assess whether exposure to pesticide residues may have a biological effect at the intestinal level, it is primarily necessary to perform in vitro exposure experiments about cell lines models of the intestinal barrier at low concentrations of the chemical. In the present study, CaCo-2 cells were exposed to different concentrations of a Deltamethrin-based commercial pesticide, which was diluted in the cell medium. An MTT viability test indicated that the cytotoxic concentration value of the pesticide inside 1 mL of medium is between 10^{-6} and 10^{-5} mL. However, the analysis of Raman spectra found that biochemical changes occur inside cells exposed to a non-cytotoxic concentration of 10^{-6} mL of the pesticide inside 1 mL of the medium. Such changes involve mainly an increase in the ratio between the amount of lipid with respect to that of the protein components in the cell cytoplasm. The results obtained by Raman micro-spectroscopy were confirmed by fluorescence images obtained by using a fluorophore staining neutral lipids. Overall, the obtained results suggest that Raman micro-spectroscopy can be successfully used to monitor the cellular modifications due to exposure at low concentrations of pesticides, as those values that can be found inside food are residuals.

Keywords: Raman micro-spectroscopy; pesticide; CaCo-2 cells

1. Introduction

Pesticides are chemicals widely used in agricultural and household environments to eliminate parasites and insects that transmit various diseases to plants, animals and humans. As a rule, they are commercially available as formulations that contain at least one active substance that allows the product to perform its action. Other substances (called coformulants) are generally added to it, in order to dissolve them more easily in water, to preserve their stability and effectiveness or to improve their penetration into the target organism. Nevertheless, the mixture of active substances and coformulants may result in increased toxicity [1]. Hence, there are rigorous limits for permissible pesticide residues in food, and also because ingestion is one of the main mechanisms by which people come into contact with pesticides. Therefore, it is of primary importance to investigate the effects of the exposure to food contaminants for human health.

Among the pesticides, pyrethroids (synthetic substances of natural origin with an insecticidal and acaricidal action) have been used for many years, mainly in agriculture [2], veterinary [3] and home pest control [4]. Their extensive use increases the exposure to these substances. Indeed, many studies pointed out that the human ingestion of pyrethroids residues through foods [5,6] and dust [7,8] increases the exposure risks with respect to the environmental inhalation pathway. In particular, Deltamethrin is one of the most important pyrethroid chemicals, because it is widely used in all the above fields, i.e., for

agricultural [9,10], veterinary [11] and household [12] scopes. Although precise rules describe the maximum concentrations of use for these substances, it has been reported that, when they are combined with each other to make mixtures, they can produce significant effects, even for concentrations below those considered safe when used individually [13]. Indeed, pyrethroids have been detected in relatively low concentrations in some fruits and vegetables [14]. Hence, it is worth investigating the effects arising after exposure to low concentrations of pesticides.

In particular, the use of in vitro models is the first step to take in order to obtain information about the effect of a xenobiotic chemical at the cellular level. In a previous work, we found that modifications of protein linkages between amino acids and, in a minor amount, lipids occurred in normal human keratinocyte cells after exposure to a commercial pesticide with a very low concentration of Deltamethrin [15]. Indeed, our previous experiment investigated the effects occurring after exposure to a pesticide by contact action. In that paper, the investigated samples were cells from the epidermitis, the outermost layer of the skin. Instead, the study of effects related to residual pesticides in food should involve cells from the intestinal tract and digestive area. In particular, the intestinal epithelial cells may be exposed to significant concentrations of these chemicals, because the intestinal barrier represents the border line between the human body and the chemicals introduced inside it with food. Therefore, epithelial cells from the intestinal barrier represent a proper model to evaluate in vitro the toxicity of food contaminants. Many cellular models replicating the human intestinal epithelium have been described in the literature to estimate cytotoxicity [16]. In particular, CaCo-2 cells have proved to be a suitable model for investigating intestinal absorption and the toxicity of xenobiotic chemicals [17]. In fact, cultured CaCo-2 cells, which arise from an immortalized cell line of human colorectal adenocarcinoma, keep the main morphological and functional characteristics of intestinal cells [16,18].

One of the first tests to be carried out to determine the admissible doses of pesticides can be obtained by estimating the viability of cell cultures exposed to these substances at different concentrations in order to identify the cytotoxic concentration, which determines the death of more than 50% of the exposed cells. However, these assays do not provide enough information about the presence of any biochemical alterations induced by the substance inside the cells that remained alive during the exposure process. For several years, Raman micro-spectroscopy has been successfully applied as a versatile tool for biomedical and bioanalytical applications [19], because of its property of providing biochemical information in a label-free manner, with easy sample preparation [20,21]. This technique allows to analyze biochemical and structural changes in the main cellular components (proteins, DNA and lipids) due to its high sensitivity in detecting modifications in the spectral signals related to the functional groups of the most important biomolecules. The potentiality of the Raman technique as a diagnostic tool for the identification of early neoplastic modifications of cells and tissues has been demonstrated in many works [22–24]. Besides the diagnostic application, Raman micro-spectroscopy has also been applied to detect biochemical changes occurring in cells in response to drug treatment [25], ionizing radiations [26], lipidomics [27], early apoptosis [28] and necrosis [29] processes.

In this work, we investigate the biochemical effect at the cellular level arising from the exposure of CaCo-2 cells to a low concentration of a commercial pesticide. After performing a viability test, we properly selected a non-cytotoxic concentration of the chemical for the exposure experiments, and we analyzed the cells before and after exposure by means of Raman micro-spectroscopy. The aim of this work is to point out that Raman micro-spectroscopy is able to detect the eventual biochemical effects that occur in CaCo-2 cells exposed to low concentrations of pesticide. This can be demonstrated by identifying any spectral biomarker that differentiates the Raman spectra of unexposed cells from those of exposed cells. Our results show that cellular modifications start after an exposure to a low concentration of the commercial pesticide. The modifications at the cytoplasmic level mainly involve the modification of the balance between lipid and protein components,

with an increase in the former with respect to the latter. This result was confirmed by fluorescence images.

2. Materials and Methods

2.1. Cell Culture and Preparation

Human colonrectal adenocarcinoma (CaCo-2) cells were obtained from ATCC (Manassas, VA, USA). They correspond to human colonrectal adenocarcinoma epithelial cells line isolated from colon tissue derived from a 72-year-old male. CaCo-2 cells were grown in Dulbecco's Modified Eagle's medium (DMEM), supplemented with 4 mmol dm^{-3} L-glutamine, 1% penicillin/streptomycin, 10% fetal bovine serum (FBS) and 1% non-essential amino acids (NEAA), at 37 °C and 5% CO_2. A commercial pesticide containing Deltamethrin as active substance was diluted using the complete medium as a solvent and obtaining serial solutions at different concentrations. Such a commercial pesticide is named as "Deca Flow 2.5". It is a concentrated insecticide in aqueous suspension, whose datasheet reports that 100 g of product contains: 2.55 g of Deltamethrin, 3.68 g of coformulants and the remaining part consists of solvent and water. Cells were seeded in 24 multi-well plates at a concentration of 7×10^3 for each well. Before exposure, the cells were washed with PBS and subsequently 1 mL of pesticide solution at different concentrations was added to each well. For each concentration, 4 samples were carried out. The cells were exposed for 24 h to different concentrations of the commercial pesticide solution, with increasing concentrations from 10^{-7} to 10^{-5} mL of pesticide inside 1 mL of medium. The concentration of the pesticide solution suggested by manufacturer for commercial use corresponds to 5×10^{-3} mL of pesticide inside 1 mL of water. The investigated concentration values are much lower with respect to the suggested value because our aim is that of studying the effects of pesticide residues on the cells from intestinal tract. The (3-(4,5-Dimethylthiazol-2-yl)-2,5-Diphenyltetrazolium Bromide) (MTT) method was used as viability test to evaluate the cytotoxic concentration of the chemical [30].

The cells to be measured by Raman micro-spectroscopy were cultured on glass coverslip after a proper poly-lysine coating was deposited on the glass surface. The cultured cells, both control and 24 h exposed, were fixed in paraformaldehyde 3.7% and stored in Petri dishes with phosphate-buffered saline (PBS) solution until Raman spectra acquisition. Each glass coverslip sample was rinsed in deionized water, in order to remove residual PBS, before Raman measurements.

2.2. Raman Spectroscopy

Raman spectra were measured by means of a Raman confocal micro-spectrometer apparatus (Labram from Jobin-Yvon Horiba, Montpellier, France), equipped with an Olympus 100× oil-immersion objective, in the range 950–3100 cm^{-1}. The 514.5 nm line of an Ar ion laser was used as exciting beam, resulting in a diffraction-limited spot focused on the sample less than 1 μm diameter. Each measured cell was excited with a laser power of 6 mW. The spectrum obtained from each single cell consisted of the average signal of three consecutive acquisitions of 10 s each one. About 40 randomly chosen cells were measured, both for control and exposed sample. The light scattered from the sample was collected in backscattering geometry. The Raman scattered light was analyzed by a diffraction grating with 600 grooves/mm and it was detected by a charge-coupled device (CCD). Before each Raman spectrum, optical images of the measured cells were obtained by a CCD camera in order to select the cellular compartment from which to measure the signal. The spectral resolution was about 5 cm^{-1}/pixel. The background signal was measured by moving the objective to coverslip regions where no cell was located.

2.3. Spectral Processing and Data Analysis

Each collected Raman spectrum was preprocessed firstly by subtracting the corresponding background signal and then by performing a subtraction of the cell fluorescence and stray light signal, described by a fifth-order polynomial function. Finally, area normalization procedure was achieved in order to normalize to the total amount of biological

material in the sampling volume. After that, an average normalized spectrum was calculated for each cell type.

PeakFit software (version 4.12, Systat Software) was used to perform deconvolution analysis of the Raman spectra. SigmaPlot software (version 12.5, Systat Software) was used to estimate the statistical differences between the two groups of different cells by means of the *t*-test method.

2.4. Fluorescence Measurements

CaCo-2 cells were seeded in 24 wells of a cell plate (Corning) at a concentration of about 5×10^4 cells/well and they were allowed to attach to the plate. Then, the culture medium was removed from four wells and a complete medium containing 100 mg ml^{-1} of oleic acid (Sigma: 03008, St. Louis, MO, USA) with 10% sterile filtered bovine serum albumin (BSA) in DPBS was placed in such four wells. Finally, the cell plate was placed for 24 h inside an incubator in order to allow lipid droplets to accumulate inside cells. Afterward, other four wells of the plate were exposed for 24 h to the pesticide at a concentration of 10^{-6} mL inside 1 mL of medium. Correspondingly, control cells were placed in other four wells. Then, the BODIPY 493–503 (D3922, Thermofisher, Waltham, MA, USA), which is a fluorescent fluorophore staining the neutral lipids, was added to the above 12 wells at a concentration of 10 µg ml^{-1}. After washing twice with DPBS, each well was fixed with *Paraformaldehyde* (PFA) solution with concentration of 3.7% in PBS and it was observed by means of an inverted optical fluorescent microscope (Olympus IX71). All experiments were performed at room temperature

3. Results

The effects of 24 h pesticide exposure on the CaCo-2 cells have been primarily evaluated by the MTT method, which assesses the cell health according to the mitochondrial activity. Based on the 50% criterion, the cytotoxic concentration corresponds to exposure to the pesticide with a concentration value between 10^{-6} and 10^{-5} mL inside 1 mL of medium, as can be deduced from Figure 1. Therefore, the 24 h exposure to the pesticide concentration of 10^{-6} mL results to be non-cytotoxic for the cells. As the aim of this work is to investigate by Raman micro-spectroscopy the eventual biochemical modifications occurring in CaCo-2 cells exposed at a pesticide concentration below the cytotoxic value, we investigated only the unexposed cells (control) and those exposed to the pesticide concentration of 10^{-6} mL. Although the viability value is 60.7% for this latter concentration, we remark that the cells measured by the Raman technique are those attached to the glass coverslip, which are alive before the fixation process (whereas most of the dead cells were detached from the coverslip).
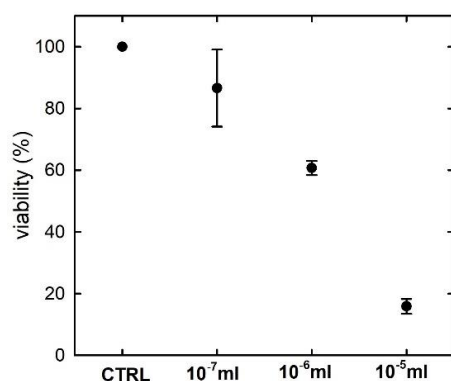

Figure 1. Results of average viability and standard deviation values of CaCo-2 cells exposed for 24 h to different concentrations of a commercial pesticide with Deltamethrin as active ingredient. The values reported on the horizontal axis refer to the volume of pesticide inside 1 mL of medium. The viability values have been obtained according to the MTT assay.

The Raman spectra of cells from the same cellular type can be slightly different because of the heterogeneity of the subcellular compartments from which the signal is measured. Therefore, the average spectra measured from many control and exposed cells should primarily be compared with each other to investigate the modifications of a cellular structure and biochemical composition as a consequence of a chemical stress. In order to discriminate signals due to different cellular components, we acquired two Raman spectra for each cell by focusing the laser beam firstly inside the nucleus and then inside the cytoplasm. In the former case, we measured the Raman signals mainly from the nucleus components (nucleic acids, DNA/RNA and proteins) and, to a lesser extent, plasmatic membrane components (mainly proteins and lipids); in the latter case, the nucleus components are excluded from the sampled volume. In this way, the comparison of the average spectra of the control and exposed cells can allow to investigate separately the similarities and differences in the nucleus and cytoplasm compartments.

In order to detect the spectral markers of specific cellular components, a comparison between the average Raman spectra of the control CaCo-2 cells, measured by focusing the laser beam inside the nucleus and inside the cytoplasm, is reported in Figure 2a,b for the 950–1750 and 2800–3100 cm^{-1} spectral ranges, respectively. The signal was not acquired below 950 cm^{-1} because a band due to the coverslip glass is located at 800 and 950 cm^{-1}: this band cannot be completely removed by means of the background subtraction procedure described in Section 2. Therefore, the presence of such a spurious and cell-to-cell variable signal could affect the area normalization process described above. The spectra in Figure 2 consist of many Raman peaks, which can be attributed according to previously published works [31]: the most prominent peaks are labeled in Figure 2 and reported in Table 1.
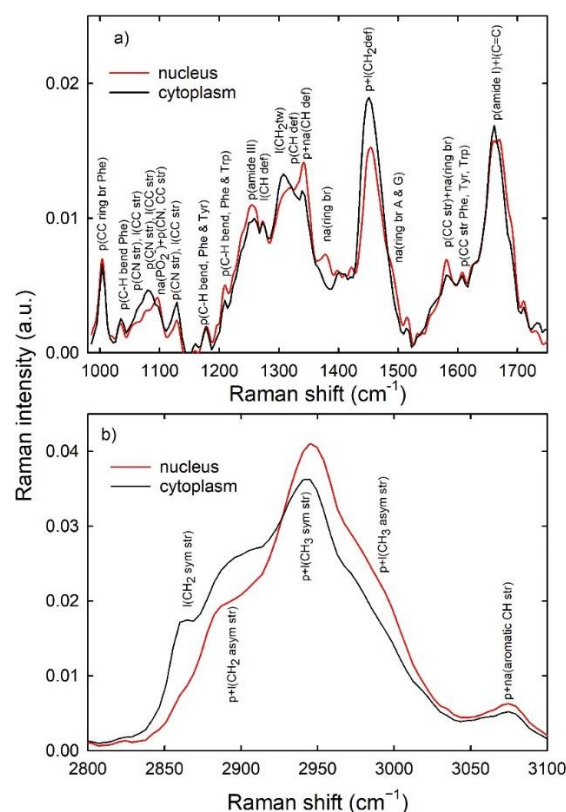

Figure 2. Average normalized Raman spectra from the cytoplasm (black lines) and nucleus (red lines) regions of control CaCo-2 cells in the 980–1750 cm^{-1} (**a**) and 2800–3100 cm^{-1} (**b**) spectral range. The attributions of the main spectral features are labeled [31]. Abbreviations: p: proteins; l: lipids; na: nucleic acids; br: breathing mode; str: stretching; bend: bending; tw: twisting; def: deformations; sym: symmetric; asym: asymmetric; Phe: phenylalanine; Tyr: tyrosine; Trp: tryptophan; A: adenine; G: guanine.

Table 1. Assignment of Raman spectral structures, according to previous results reported in literature [31] and in the present investigation. Abbreviations: Phe: phenylalanine, Tyr: tyrosine, Trp: tryptophan, p.: proteins, l.: lipids, d: DNA backbone, n.a: DNA bases, str: stretching, bend: bending, def: deformation, wagg: wagging, twist: twisting, sciss: scissoring. The highlighted peaks will be investigated by ratiometric analysis (see text).

Spectral Position (cm^{-1})	Assignment
1003	(ring breathing, Phe)
1035	(C-H in-plane bend., Phe)
1060	(C-N str., p.) + (C-C str., l.)
1080–1095	(PO_2^- str., d) + (C-N str., p.) + (C-C str., p.)
1130	(C-N str., p.) + (C-C str., l.)
1180	(C-H bend., Tyr, Phe)
1210	(C-H bend., Trp, Phe)
1260–1270	(Amide III, p.)
1280	(C-H def., l.)
1300–1320	(CH_2 twist., l.) + (CH_3 def., CH_2 wagg., p.)
1340	(CH_3 def., CH_2 wagg., p. and n.a.)
1380	(ring breathing, n.a.)
1450	(CH_2 sciss., l.) + (CH_2 sciss., p.)
1480	(ring breathing, n.a.)
1580	(ring breathing, n.a.) + (C=C str., p.)
1610	(C=C str., Phe, Tyr., Trp.)
1660	(Amide I, p.) + (C=C str., l.)
2858	(CH_2 symmetric stretching, l.)
2890	(CH_2 asymmetric stretching, p.+l.)
2940	(CH_3 symmetric stretching, p.+l.)
2980	(CH_3 asymmetric stretching, p.+l.)

The main spectral differences between the nucleus and cytoplasm spectra are related to a large contribution of the vibrational modes of DNA and nucleic acids in the former (red lines) and to an important influence of the peaks involving the lipid in the latter (black lines). However, the major Raman peaks in both spectra are related to the protein vibrational modes, specifically amide I (at about 1660 cm^{-1}), amide III (at about 1260–1270 cm^{-1}), CH (at 1320 and 1340 cm^{-1}) and CH_2 (at 1450 cm^{-1}) bending, the ring breathing of the Phenylalanine (at 1003 cm^{-1}), CC (at 1060, 1082, 1580, 1610 cm^{-1}) and CN (1060, 1082 and 1130 cm^{-1}) stretching modes, the asymmetric CH_2 stretching modes (at about 2890 cm^{-1}) and the symmetric and asymmetric CH_3 stretching modes (at 2940 and about 2980 cm^{-1}, respectively). In the spectrum sampling cytoplasm, well-resolved lipid vibrational peaks are observed at 1305 cm^{-1} (CH_2 bending) and at about 2858 cm^{-1} (CH_2 symmetric stretching), although the lipid contribution to the Raman spectrum is overlapped to the protein signal at 1060, 1082, 1130, 1450, 1660, 2940 and 2980 cm^{-1}. Instead, the nucleic acids and DNA/RNA peaks are overlapped to protein peaks in the spectrum sampling nucleus, particularly at 1095 cm^{-1} (PO_2^- phosphodioxy bond of phosphate group), 1340 cm^{-1} (CH bending), 1380 and 1580 cm^{-1} (ring breathing of DNA/RNA bases).

The spectra in Figure 2 are very similar to those measured by K. Beton et al. for different cellular compartments of CaCo-2 cells [32–34], except for the relative intensity of the amide I peak, which is quite large with respect to the intensity of the spectra in Figure 2. Probably, this is due to the background subtraction procedure which, in our case, slightly decreases the intensity of the amide I peak, because of the small Raman peak due to the OH bending of water at 1640 cm^{-1} [35]. In fact, our spectra are more similar, particularly where the fingerprint region is concerned, to those measured by R. Algazheer et al. about a freeze-dried pellet of CaCo-2 cells [36]. Instead, the spectra in Figure 2 are quite different

from those measured by A.F.D. de Namor et al., although these last authors did not provide any information about the pretreatment of the measured Raman data [37].

The normalized and average Raman spectra measured from the nucleus and cytoplasm compartments of the control and exposed CaCo-2 cells are shown in Figure 3a,b, respectively. Most features of these Raman spectra are very similar, but several of them showed small visual differences from the control to the exposed cells. In particular, it is evident in Figure 3a that the intensity of the nucleic acids-related signals at 1340, 1380 and 1580 cm^{-1}, as well as that of a few protein-related signals at 1260 and 1320 cm^{-1}, is lower in the exposed cells than in the control ones, whereas some protein-related features at 1003, 1130, 1320, 1610, 1660, 2900 and 2945 cm^{-1} are characterized by a larger intensity in the exposed than in the control cells. Correspondingly, Figure 3b emphasizes the intensity decrease in the protein-related peaks at 1260, 1340, 1580 and 3070 cm^{-1} in the exposed cells with respect to the control ones, whereas the intensity of the lipid peak at 2858 cm^{-1} increases in the exposed cells and that of the lipid peak at 1305 cm^{-1} is almost unchanged for the two types of samples. In addition, all the Raman peaks related to the overlapping contribution of the proteins and lipids is larger in the exposed cells than in the control ones. Therefore, these intensity changes suggest that the chemical exposure causes biochemical modifications in the intracellular environment, although the exposure concentration is at a lower level than that of the cytotoxic one. Nonetheless, Raman micro-spectroscopy is able to detect such biochemical modifications.
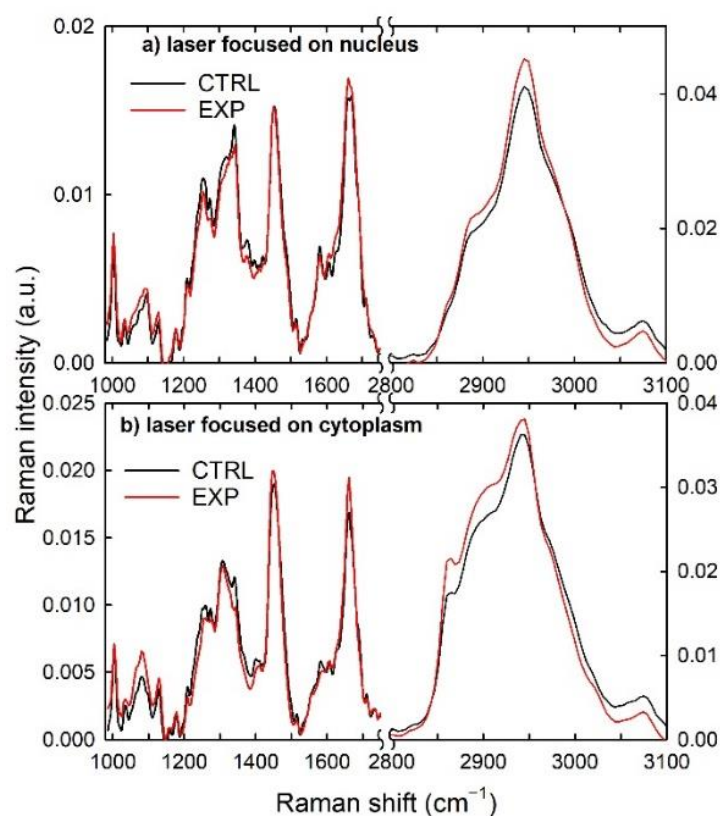

Figure 3. Comparison between average normalized Raman spectra measured from the nucleus (**a**) and cytoplasm (**b**) regions of control (black lines) and exposed (red lines) CaCo-2 cells.

However, it is not clearly evident in Figure 3 what cellular components and bonds are mostly modified by the action of the chemical. In order to further investigate such an issue, it has to be remarked that Figure 3 shows the comparison between normalized spectra: as a consequence, it is scarcely helpful to consider the intensity change in a given Raman peak from the control to the exposed spectrum. Instead, the ratio between the relative intensities

of two or more specific Raman peaks has to be analyzed. For this purpose, it is essential to properly select the Raman peaks whose intensity ratios should be analyzed.

In particular, the spectra measured in the region of the nucleus could provide information about the influence of the chemical on the components related to nucleic acids and proteins by investigating the modification of the ratio between the intensities of specific Raman peaks related to these components. In fact, nucleic acids and proteins mainly characterize the Raman spectra acquired in the nucleus region, while spectral structures due to lipids are scarcely visible and resolved. Therefore, as an index of the modification of the nucleic acids-related components compared to the proteins-related ones in the nucleus region, we can consider the ratio between the intensity of the peak at 1340 cm^{-1}, due to the CH deformation vibrations both in the proteins and in the nucleic acids, with respect to the intensity of the peak at 1320 cm^{-1}, due to the vibrational modes of the CH deformation related exclusively to the proteins. The choice of this ratio (I_{1340}/I_{1320}) is because the Raman peak at 1340 cm^{-1} has the largest intensity among those related to the vibrational modes of the nucleic acids.

Instead, the Raman spectra measured on the cytoplasm region can be used to evaluate the action of the chemical on the lipids and proteins present in this subcellular compartment. In this case, to compare the effects of the Deltamethrin-based pesticide on these two cellular components, the intensity ratios of various Raman peaks whose intensities are relatively large can be considered. The spectral position of such Raman peaks is highlighted in grey in Table 1. In particular, the following three intensity ratios can be analyzed to estimate the changes that occurred in the lipid component with respect to the protein component: *(i)* the ratio (I_{2858}/I_{2940}) between the intensity of the peak at 2858 cm^{-1}, due to the CH$_2$ symmetric stretching of the lipids, with respect to the intensity of the peak at 2940 cm^{-1}, due to the CH$_3$ symmetric stretching of both the proteins and lipids; *(ii)* the ratio (I_{1305}/I_{1340}) between the intensity of the peak at 1305 cm^{-1}, due to the CH$_2$ twisting of the lipids, with respect to the intensity of the peak at 1340 cm^{-1}, due to the CH deformation vibration of the proteins; and *(iii)* the ratio ($I_{1450}/I_{amideIII}$) between the intensity of the peak at 1450 cm^{-1}, due to the CH$_2$ deformation vibration of both the lipids and proteins, with respect to the intensity of the peak at about 1260 cm^{-1}, due to the amide III vibrational mode of the proteins.

A ratiometric analysis of vibrational spectra has been successfully used for many years for the interpretation of results from spectral measurements. Many works have shown that it could be promising for application in disease diagnosis [38]. The intensity ratio of many Raman peaks has been analyzed for investigating the effect of the chemical or physical stress on a cellular sample, as well as the different stages of pathology [38]. Our choice of the above ratios was made according to three factors, i.e., the choice of *(i)* the relatively large intensity peaks involved in the ratio; *(ii)* well-resolved peaks; and *(iii)* the ratio between two peaks, where at least one of the two is related to only one type of the main cellular components (nucleic acids, proteins or lipids).

In order to estimate the above intensity ratios, we achieved a deconvolution analysis of each measured spectrum in the spectral range, including the above Raman peaks, as shown in Figure 4, for the Raman spectrum collected from the cytoplasm region of a typical control CaCo-2 cell. In particular, each spectrum was fitted by means of Voigt functions, consisting of overlapped Gaussian and Lorentzian functions [39,40]. For each fitting procedure, the spectral positions of the fitting functions were fixed, according to the minima of the second derivative function of the experimental spectrum. Such a step was performed in order to minimize the fitting parameters and to make the fit as reliable as possible. Fitting procedures by means of Voigt functions have been reported by G. Pezzotti as a very useful tool for the deconvolution of Raman spectra in cell biology and microbiology [21]. However, other functions, such as Lorentzian [41] and Gaussian [42] ones, have been reported. We used Voigt functions because they better fit the Raman spectra than Lorentzian and Gaussian functions.
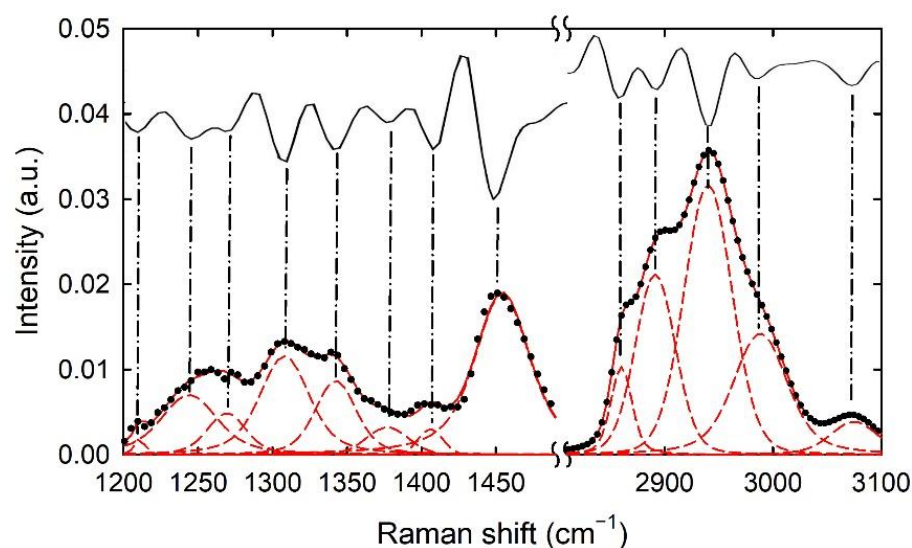
Figure 4. Typical Raman spectrum of control CaCo-2 cells (black dots) with deconvolution analysis by means of Voigt functions. The single Raman peaks are shown by red dash lines, whereas the sum of the Raman peaks corresponds to the continuous red line. The spectral position of the Raman peaks has been deduced by minima of second derivative spectra (continuous black lines), as indicated by dash-dotted lines.

After the deconvolution procedure, the areas of the specific Voigt functions related to the Raman peaks above, selected for estimating the effects of the chemical on the cellular components, were calculated. Therefore, the intensity ratios I_{1340}/I_{1320} for the nucleus region and I_{2858}/I_{2940}, I_{1305}/I_{1340} and $I_{1450}/I_{amideIII}$ were estimated according to the areas of the corresponding Raman peaks. The investigated area ratios are reported in Figure 5. The action of the chemical at the nucleus level causes a slight decrease in the intensity of the nucleic acids peak with respect to that of the protein one, as visible in Figure 5a. However, the I_{1340}/I_{1320} area ratio values of the control cells are not statistically significantly different from those of the exposed cells. Hence, it can be deduced that the action of the chemical is mild at the nucleus level so that the balance between the main cellular components of the nucleus is only slightly modified, where the nucleic acid bonds are more altered than the protein bonds. Such a result is in good agreement with what R. Alghazeer et al. have found about the decrease in the intensity of the 1336 cm^{-1} peak with respect to that of the amide III band for the Raman spectra of CaCo-2 cells exposed to polyunsaturated fatty acids in comparison with the Raman spectra of control cells [36]. In particular, these authors found a large and statistically significant decrease in the above intensity peaks ratio. Probably, this is due to the large concentration of the investigated chemical (100 µg/mL methyl linoleate or fish oil), whereas in our case, the chemical concentration is well lower than the cytotoxic value.

On the contrary, Figure 5b–d clearly highlight that the balance between the lipid and protein components in the cytoplasm region is definitely modified, as can be deduced from the largely significant difference between the I_{2858}/I_{2940}, I_{1305}/I_{1340} and $I_{1450}/I_{amideIII}$ for the control and exposed cells. The values of all three investigated area ratios are larger in the exposed than in the control cells. This result is in strong disagreement with that of R. Alghazeer et al., because they found a decrease in the intensity ratio of the 1302 cm^{-1} Raman peak with respect to the amide III band, after the exposure of the CaCo-2 cells to polyunsaturated fatty acids [35]. However, these authors exposed the CaCo-2 cells to a large concentration of chemical, as reported above, so that lipid peroxidation occurred with a dramatic injury to the plasmatic membrane (which they confirmed by means of atomic force microscopy images).
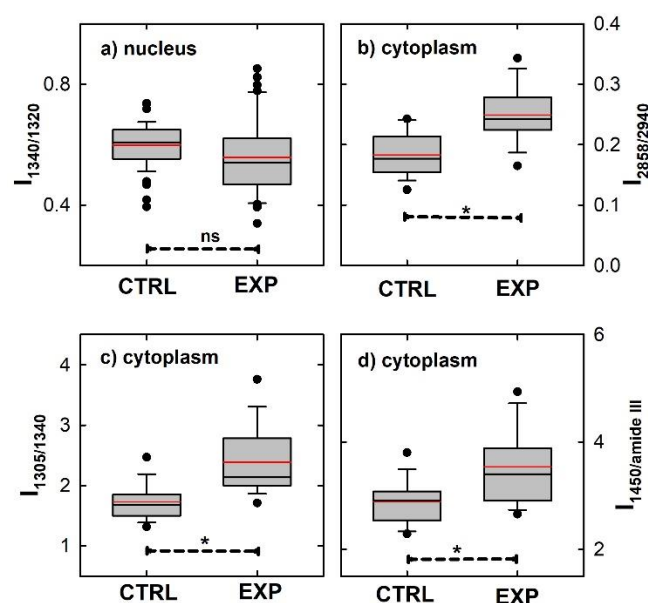
Figure 5. Box plots reporting the comparison of the area ratios for selected peaks, related to different cellular components, in the normalized Raman spectra of control and exposed CaCo-2 cells. In (**a**), the ratio between the area of the peak centered at about 1340 cm^{-1} (related to CH deformation of protein and nucleic acid components) with respect to the area of the peak at 1320 cm^{-1} (related to protein components) for spectra from nucleus region is reported; in (**b**), the ratio between the areas of the peak centered at about 2858 cm^{-1} (related to lipid components) with respect to the area of the peak at 2940 cm^{-1} (related to both protein and lipid components) for spectra from cytoplasm region is shown; in (**c**), the ratio between the area of the peak centered at about 1305 cm^{-1} (related to lipid components) with respect to the area of the peak at 1340 cm^{-1} (related to protein components) for spectra from cytoplasm region is displayed; in (**d**), the ratio between the area of the peak centered at about 1450 cm^{-1} (related to both lipid and protein components) with respect to the area of the peak of amide III at about 1260 cm^{-1} (related to protein components) for spectra from cytoplasm region appears. Mean and median values are shown with red and black lines, respectively, inside each box. Whiskers correspond to 5th and 95th percentiles and black dots correspond to outliers. The statistically significant differences among each group of cells (dashed lines, ns indicating not significant, while * indicating statistical significance with $p < 0.001$) were estimated by means of Anova test.

Therefore, our Raman data suggest that the action of the chemical substance at a low concentration is mainly limited at the cytoplasmic level and involves a modification of the balance between the lipid and protein components, due to an increase in lipids with respect to proteins or a decrease in proteins with respect to lipids. The analysis of the normalized Raman spectra cannot specify precisely which one of the two previous cases occurs.

To try to get more insight about lipids modifications in exposed cells with respect to control ones, we performed an assessment of the lipid content inside CaCo-2 cells by means of fluorescence images, after the cells' exposure to the pesticide with the investigated concentration. In particular, we obtained fluorescence images by using the fluorophore BODIPY (D-3922), which is targeted to quantify neutral lipids and lipid droplets content. From typical fluorescence images, shown in Figure 6, it can be deduced that the fluorescence increases from the control (Figure 6a) to the 5×10^{-8} M exposed (Figure 6b) cells, because of the increase in neutral lipid synthesis. In particular, the fluorescence intensity from the exposed cells is similar to that from oleic acid exposed cells (Figure 6c). Oleic acid usually serves as a positive control for increased neutral lipid content because it is known to be an inducer of triglyceride synthesis and storage [43].
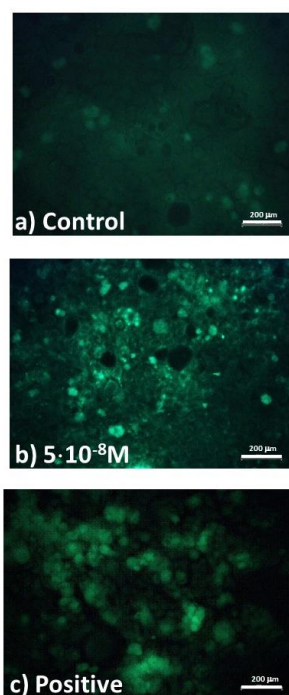
Figure 6. Fluorescence of (**a**) control cells and (**b**) cells exposed to a commercial pesticide concentration of 10^{-6} mL inside 1 mL of medium, after exposure to BODIPY 493–503 nm having a concentration of 10 µg·mL^{-1} at room temperature. Cells exposed to oleic acid (positive control) are shown in (**c**). The scale bars correspond to 200 µm.

Therefore, the modifications of the lipid-to-protein ratio in the cell cytoplasm, observed by means of Raman micro-spectroscopy, correspond to an increase in the lipids amount with respect to the proteins amount and it might be related to a response of the cells to the modifications related to the pesticide action, with the formation of lipid droplets. The increased lipid droplets could have a probable role in repairing the damage of the membrane as a consequence of the pesticide action [44,45].

4. Conclusions

The obtained results point out that Raman micro-spectroscopy measurements and the ratiometric analysis of spectra are able to highlight cellular modifications occurring inside the cytoplasm of CaCo-2 cells, a model of epithelial cells from the intestinal barrier, after exposure at a non-cytotoxic concentration of a Deltamethrin-based commercial pesticide. In particular, such modifications, mainly concerning the increase in the amount of the lipid component with respect to the protein one, are not enough to cause cell death, because they are measured in cells that are alive following exposure. Probably, the increase in the lipid component amount is related to the formation of lysosomal vesicles which bind to the plasmatic membrane in order to activate membrane repair mechanisms, which are needed after the membrane damage caused by the pesticide action. Regardless, in the investigated topic, the increased intensity of lipid peaks can be considered a spectral biomarker of the residual pesticide exposure at the intestinal level.

Raman micro-spectroscopy has several advantages with respect to other conventional tests for evaluating biochemical damage (viability, senescence, fluorescence, apoptosis and necrosis assays, etc.). In fact, most biological assays are time-consuming and/or they are based on the use of expensive and non-physiological chemicals, such as reagents, antibodies and dyes. On the contrary, the Raman technique requires little time for the preparation of the sample, it is label-free and allows the simultaneous detection of several cellular components, with samples that are not destroyed by the measurement procedure.

In addition, the Raman technique is able to yield information at the single-cell level, unlike many biological assays.

However, some drawbacks need to be properly addressed and solved before the Raman technique can be routinely used in biomedical laboratories to achieve a biochemical analysis at the cellular, tissue or biofluid level. Indeed, the signal collection efficiency needs to be optimized, because weak Raman signals can lead to a long acquisition time. Moreover, substrate and sample auto-fluorescence can overwhelm the Raman signal, so a proper background subtraction procedure should be optimized and standardized. In addition, in most cases, the biological molecules inside investigated samples are minimally affected by the chemical and/or physical stress process or by the onset of pathology, so a sophisticated procedure for a spectra analysis is required (ratiometric analysis, multivariate analysis, etc.) to emphasize the biochemical modifications.

Eventually, the Raman approach proved to be highly sensitive for the detection of the pesticide effect at an exposure concentration lower than that of the cytotoxic value. Although the exposure at a low concentration is not enough for the cell death nor for the onset of typical cellular processes, such as apoptosis and lipid peroxidation, it is able to cause cellular modifications which could evolve toward cellular pathologies. In addition, the Raman technique can be also used as a complementary diagnostic method in the cases from mild-to-moderate pesticide overexposures, when a nonspecific clinical presentation occurs. Such cases are mainly found in agricultural workers. Hence, Raman biomarkers for exposure could be applied in epidemiological studies in order to improve our understanding of the health effects of pesticide exposure in both the short and long term.

References

1. Karaca, M.; Fischer, B.C.; Willenbockel, C.T.; Tralau, T.; Marx-Stoelting, P.; Bloch, D. Effects of co-formulants on the absorption and secretion of active substances in plant protection products in vitro. *Arch. Toxicol.* **2021**, *95*, 3205–3221. [CrossRef]
2. Singh, S.; Mukherjee, A.; Jaiswal, D.K.; Pereira, A.P.D.A.; Prasad, R.; Sharma, M.; Kuhad, R.C.; Shukla, A.C.; Verma, J.P. Advances and future prospects of pyrethroids: Toxicity and microbial degradation. *Sci. Total Environ.* **2022**, *829*, 154561. [CrossRef] [PubMed]
3. Anadón, A.; Arés, I.; Martínez, M.A.; Martínez-Larrañaga, M.R. Pyrethrins and Synthetic Pyrethroids: Use in Veterinary Medicine. In *Natural Products*; Ramawat, K., Mérillon, J.M., Eds.; Springer: Berlin/Heidelberg, Germany, 2013.
4. Class, T.J.; Kintrup, J. Pyrethroids as household insecticides: Analysis, indoor exposure and persistence. *Anal. Bioanal. Chem.* **1991**, *340*, 446–453. [CrossRef]
5. Shi, Y.-H.; Xiao, J.-J.; Feng, R.-P.; Liu, Y.-Y.; Liao, M.; Wu, X.-W.; Hua, R.-M.; Cao, H.-Q. In-vitro bioaccessibility of five pyrethroids after human ingestion and the corresponding gastrointestinal digestion parameters: A contribution for human exposure assessments. *Chemosphere* **2017**, *182*, 517–524. [CrossRef]
6. Kuang, L.; Hou, Y.; Huang, F.; Hong, H.; Sun, H.; Deng, W.; Lin, H. Pesticide residues in breast milk and the associated risk assessment: A review focused on China. *Sci. Total Environ.* **2020**, *727*, 138412. [CrossRef]
7. Figueiredo, D.M.; Nijssen, R.; Krop, E.J.; Buijtenhuijs, D.; Gooijer, Y.; Lageschaar, L.; Duyzer, J.; Huss, A.; Mol, H.; Vermeulen, R.C. Pesticides in doormat and floor dust from homes close to treated fields: Spatio-temporal variance and determinants of occurrence and concentrations. *Environ. Pollut.* **2022**, *301*, 119024. [CrossRef]
8. Wang, J.; Lin, K.; Taylor, A.; Gan, J. In vitro assessment of pyrethroid bioaccessibility via particle ingestion. *Environ. Int.* **2018**, *119*, 125–132. [CrossRef]

9. Housset, P.; Dickmann, R. A promise fulfilled-pyrethroid development and the benefits for agriculture and human health. *Bayer CropScience J.* **2009**, *62*, 135–144.
10. Bhanu, S.; Archana, S.; Ajay, K.; Bhatt, J.L.; Bajpai, S.P.; Singh, P.S.; Vandana, B. Impact of deltamethrin on environment, use as an insecticide and its bacterial degradation-a preliminary study. *Int. J. Environ. Sci.* **2011**, *1*, 977.
11. Elias, P. The Use of Deltamethrin on Farm Animals. In *Insecticides—Development of Safer and More Effective Technologies*; IntechOpen: London, UK, 2013.
12. Cao, X.M.; Song, F.L.; Zhao, T.Y.; Dong, Y.D.; Sun, C.X.; Lu, B.L. Survey of Deltamethrin Resistance in House Flies (*Musca domestica*) from Urban Garbage Dumps in Northern China. *Environ. Èntomol.* **2006**, *35*, 1–9. [CrossRef]
13. Kortenkamp, A.; Faust, M.; Scholze, M.; Backhaus, T. Low-level exposure to multiple chemicals: Reason for human health concerns? *Environ. Health Perspect.* **2007**, *115* (Suppl. S1), 106–114. [CrossRef] [PubMed]
14. Lu, C.; Schenck, F.J.; Pearson, M.A.; Wong, J.W. Assessing Children's Dietary Pesticide Exposure: Direct Measurement of Pesticide Residues in 24-Hr Duplicate Food Samples. *Environ. Health Perspect.* **2010**, *118*, 1625–1630. [CrossRef] [PubMed]
15. Perna, G.; Lasalvia, M.; Capozzi, V. Raman microspectroscopy discrimination of single human keratinocytes exposed at low dose of pesticide. *J. Mol. Struct.* **2012**, *1010*, 123–129. [CrossRef]
16. Fedi, A.; Vitale, C.; Ponschin, G.; Ayehunie, S.; Fato, M.; Scaglione, S. In vitro models replicating the human intestinal epithelium for absorption and metabolism studies: A systematic review. *J. Control. Release* **2021**, *335*, 247–268. [CrossRef] [PubMed]
17. Sambuy, Y.; De Angelis, I.; Ranaldi, G.; Scarino, M.L.; Stammati, A.; Zucco, F. The Caco-2 cell line as a model of the intestinal barrier: Influence of cell and culture-related factors on Caco-2 cell functional characteristics. *Cell Biol. Toxicol.* **2005**, *21*, 1–26. [CrossRef]
18. Le Ferrec, E.; Chesne, C.; Artusson, P.; Brayden, D.; Fabre, G.; Gires, P.; Guillou, F.; Rousset, M.; Rubas, W.; Scarino, M.L. In Vitro models of the intestinal barrier: The report and recommendations of ECVAM Workshop 46. *Altern. Lab. Anim.* **2001**, *29*, 649–668. [CrossRef]
19. Pappas, D.; Smith, B.W.; Winefordner, J.D. Raman spectroscopy in bioanalysis. *Talanta* **2000**, *51*, 131–144. [CrossRef]
20. Matthäus, C.; Bird, B.; Miljković, M.; Chernenko, T.; Romeo, M.; Diem, M. Infrared and Raman microscopy in cell biology. *Methods Cell Biol.* **2008**, *89*, 275–308.
21. Pezzotti, G. Raman spectroscopy in cell biology and microbiology. *J. Raman Spectrosc.* **2021**, *52*, 2348–2443. [CrossRef]
22. Almond, L.M.; Hutchings, J.; Shepherd, N.; Barr, H.; Stone, N.; Kendall, C. Raman spectroscopy: A potential tool for early objective diagnosis of neoplasia in the oesophagus. *J. Biophotonics* **2011**, *4*, 685–695. [CrossRef]
23. Ramos, I.R.M.; Malkin, A.; Lyng, F.M. Current Advances in the Application of Raman Spectroscopy for Molecular Diagnosis of Cervical Cancer. *BioMed Res. Int.* **2015**, *2015*, 561242. [CrossRef] [PubMed]
24. Sharma, N.; Takeshita, N.; Ho, K.Y. Raman Spectroscopy for the Endoscopic Diagnosis of Esophageal, Gastric, and Colonic Diseases. *Clin. Endosc.* **2016**, *49*, 404–407. [CrossRef] [PubMed]
25. Czaja, M.; Skirlińska-Nosek, K.; Adamczyk, O.; Sofińska, K.; Wilkosz, N.; Rajfur, Z.; Szymoński, M.; Lipiec, E. Raman Research on Bleomycin-Induced DNA Strand Breaks and Repair Processes in Living Cells. *Int. J. Mol. Sci.* **2022**, *23*, 3524. [CrossRef] [PubMed]
26. Harder, S.J.; Matthews, Q.; Isabelle, M.; Brolo, A.G.; Lum, J.J.; Jirasek, A. A Raman Spectroscopic Study of Cell Response to Clinical Doses of Ionizing Radiation. *Appl. Spectrosc.* **2015**, *69*, 193–204. [CrossRef] [PubMed]
27. Wu, H.; Volponi, J.V.; Oliver, A.E.; Parikh, A.N.; Simmons, B.A.; Singh, S. In vivo lipidomics using single-cell Raman spectroscopy. *Proc. Natl. Acad. Sci. USA* **2011**, *108*, 3809–3814. [CrossRef]
28. Czamara, K.; Petko, F.; Baranska, M.; Kaczor, A. Raman microscopy at the subcellular level: A study on early apoptosis in endothelial cells induced by Fas ligand and cycloheximide. *Analyst* **2016**, *141*, 1390–1397. [CrossRef]
29. Ong, Y.H.; Lim, M.; Liu, Q. Comparison of principal component analysis and biochemical component analysis in Raman spectroscopy for the discrimination of apoptosis and necrosis in K562 leukemia cells. *Opt. Express* **2012**, *20*, 22158–22171. [CrossRef]
30. van Meerloo, J.; Kaspers, G.J.L.; Cloos, J. Cell sensitivity assays: The MTT assay. In *Cancer Cell Culture. Methods in Molecular Biology (Methods and Protocols)*; Cree, I., Ed.; Humana Press: Totowa, NJ, USA, 2011; Volume 731.
31. Talari, A.C.S.; Movasaghi, Z.; Rehman, S.; Rehman, I.U. Raman Spectroscopy of Biological Tissues. *Appl. Spectrosc. Rev.* **2014**, *50*, 46–111. [CrossRef]
32. Beton, K.; Wysocki, P.; Brozek-Pluska, B. Mevastatin in colon cancer by spectroscopic and microscopic methods—Raman imaging and AFM studies. *Spectrochim. Acta Part A Mol. Biomol. Spectrosc.* **2021**, *270*, 120726. [CrossRef]
33. Brozek-Pluska, B.; Beton, K. Oxidative stress induced by tBHP in human normal colon cells by label free Raman spectroscopy and imaging. The protective role of natural antioxidants in the form of β-carotene. *RSC Adv.* **2021**, *11*, 16419–16434. [CrossRef]
34. Brozek-Pluska, B. Statistics assisted analysis of Raman spectra and imaging of human colon cell lines–Label free, spectroscopic diagnostics of colorectal cancer. *J. Mol. Struct.* **2020**, *1218*, 128524. [CrossRef]
35. Wang, Z.; Pakoulev, A.; Pang, Y.; Dlott, D.D. Vibrational Substructure in the OH Stretching Transition of Water and HOD. *J. Phys. Chem. A* **2004**, *108*, 9054–9063. [CrossRef]
36. Alghazeer, R.; Burwaiss, A.A.; Howell, N.K.; Alansari, W.S.; Shamlan, G.; Eskandrani, A.A. Determining the Cytotoxicity of Oxidized Lipids in Cultured Caco-2 Cells Using Bioimaging Techniques. *Molecules* **2020**, *25*, 1693. [CrossRef] [PubMed]
37. Danil de Namor, A.F.; Al Hakawati, N.; Farhat, S.Y. Targeting Colorectal Cancer Cells with a Functionalised Calix [4] arene Receptor: Biophysical Studies. *Molecules* **2022**, *27*, 510. [CrossRef]
38. Kumar, S.; Verma, T.; Mukherjee, R.; Ariese, F.; Somasundaram, K.; Umapathy, S. Raman and infra-red microspectroscopy: Towards quantitative evaluation for clinical research by ratiometric analysis. *Chem. Soc. Rev.* **2016**, *45*, 1879–1900. [CrossRef]

39. Sadat, A.; Joye, I.J. Peak Fitting Applied to Fourier Transform Infrared and Raman Spectroscopic Analysis of Proteins. *Appl. Sci.* **2020**, *10*, 5918. [CrossRef]

40. Chen, Y.; Dai, L. Automated decomposition algorithm for Raman spectra based on a Voigt line profile model. *Appl. Opt.* **2016**, *55*, 4085–4094. [CrossRef]

41. Delfino, I.; Perna, G.; Lasalvia, M.; Capozzi, V.; Manti, L.; Camerlingo, C.; Lepore, M. Visible micro-Raman spectroscopy of single human mammary epithelial cells exposed to x-ray radiation. *J. Biomed. Opt.* **2015**, *20*, 035003. [CrossRef]

42. Gullekson, C.; Lucas, L.; Hewitt, K.; Kreplak, L. Surface-Sensitive Raman Spectroscopy of Collagen I Fibrils. *Biophys. J.* **2011**, *100*, 1837–1845. [CrossRef]

43. Qiu, B.; Simon, M.C. BODIPY 493/503 staining of neutral lipid droplets for microscopy and quantification by flow cytometry. *Bio-Protocol* **2016**, *6*, e1912. [CrossRef]

44. Andrews, N.W.; Corrotte, M. Plasma membrane repair. *Curr. Biol.* **2018**, *28*, R392–R397. [CrossRef] [PubMed]

45. Lasalvia, M.; Ambrico, M.; Ligonzo, T.; Perna, G.; Ambrico, P.F.; Capozzi, V. Keratinocyte cellular damage induced by pesticide doses below the cytotoxic level evidenced by electrical impedance and broadband dielectric spectroscopy. *J. Phys. D Appl. Phys.* **2022**, *55*, 125402. [CrossRef]